



# Variability in manometric sea level from reanalyses and observation-based products over the Arctic and North Atlantic oceans and the Mediterranean Sea

Andrea Storto<sup>1</sup>, Giulia Chierici<sup>1</sup>, Julia Pfeffer<sup>2</sup>, Anne Barnoud<sup>2</sup>, Romain Bourdalle-Badie<sup>3</sup>,  
Alejandro Blazquez<sup>4</sup>, Davide Cavaliere<sup>1</sup>, Noémie Lalau<sup>2</sup>, Benjamin Coupry<sup>2</sup>, Marie Drevillon<sup>3</sup>,  
Sebastien Fourest<sup>4</sup>, Gilles Larnicol<sup>2</sup>, and Chunxue Yang<sup>1</sup>

<sup>1</sup>Institute of Marine Sciences (ISMAR), National Research Council (CNR), 00133 Rome, Italy

<sup>2</sup>Magellium, 31520 Ramonville-Saint-Agne, France

<sup>3</sup>Mercator Ocean International (MOI), 31400 Toulouse, France

<sup>4</sup>Laboratory of Space Geophysical and Oceanographic Studies (LEGOS), 31401 Toulouse, France

**Correspondence:** Andrea Storto (andrea.storto@cnr.it)

Received: 2 August 2023 – Discussion started: 29 August 2023

Revised: 25 July 2024 – Accepted: 16 August 2024 – Published: 30 September 2024

**Abstract.** Regional variations in the mass component of sea level (manometric sea level) are intimately linked with the changes in the water cycle, volume transports, and inter-basin exchanges. Here, we investigate the consistency at the regional level of the manometric sea level from the Copernicus Marine Service Global Reanalysis Ensemble Product (GREP) and compare with observation-based products deduced from either gravimetry (GRACE missions) or altimetry and in situ ocean observations (sea level budget, SLB, approach) for some climate-relevant diagnostics such as interannual variability, trends, and seasonal amplitude. The analysis is performed for three basins (the Mediterranean Sea and Arctic and North Atlantic oceans) and indicates very different characteristics across the three. The Mediterranean Sea exhibits the largest interannual variability, the Arctic Ocean the largest trends, and the North Atlantic a nearly linear increase that is highly correlated to global barystatic sea level variations. The three datasets show significant consistency at both the seasonal and the interannual timescales, although the differences in the linear trends are sometimes significant (e.g. GRACE overestimates the trend in the Arctic and underestimates it in the Mediterranean Sea when compared to the other products). Furthermore, the Gravity Recovery and Climate Experiment (GRACE) and GREP data prove to be mutually more consistent than SLB in most cases. Finally, we analyse the main modes of climate variability affecting the manometric sea level variations over the selected ocean basins through regularised regression; the North Pacific Gyre Oscillation, the Arctic Oscillation, and the Atlantic Multidecadal Oscillation are proven to be the most influential modes for the North Atlantic Ocean, Mediterranean Sea, and Arctic Ocean manometric sea levels, respectively.

## 1 Introduction

Contemporary changes in global sea level are driven mostly by two contributions. The first is density-driven variations in the sea level, the so-called steric sea level that responds to the expansion and contraction of seawater due, mostly, to increasing heat in the oceans (Storto et al., 2019a). The other contributor to global sea level change is the ocean mass

change, called the barystatic sea level (Gregory et al., 2019). The barystatic sea level has been recently found to be responsible for the majority (about 60%) of the global sea level changes (Frederikse et al., 2020; Fox-Kemper et al., 2021). Recent estimates indicate  $2.25 \pm 0.16 \text{ mm yr}^{-1}$  of sea level rise due to barystatic changes for the recent period (2005–2016; Amin et al., 2020). Changes in the barystatic sea level are due to the loss of mass from glaciers and ice sheets

**Table 1.** Product table.

Product ref. no	Product ID and type	Data access	Documentation
1	GLOBAL_MULTIYEAR_PHY_ENS_001_031 (GREP), numerical models	EU Copernicus Marine Service Product (2022a)	QUID (quality information document): Desportes et al. (2022) PUM (product user manual): Gounou et al. (2022)
2	Barystatic and manometric from satellite gravimetry (LEGOS – MAGELLIUM)	Magellium/LEGOS (2023a): <a href="https://doi.org/10.24400/527896/A01-2023.011">https://doi.org/10.24400/527896/A01-2023.011</a>	PUM (product user manual): <a href="https://www.aviso.altimetry.fr/fileadmin/documents/data/products/indic/WAMBOR-DT-009-MAG_CopernicusMarine_ServiceEvolution_PUM_v2.0.pdf">https://www.aviso.altimetry.fr/fileadmin/documents/data/products/indic/WAMBOR-DT-009-MAG_CopernicusMarine_ServiceEvolution_PUM_v2.0.pdf</a> *
3	Barystatic and manometric from sea level budget (LEGOS and MAGELLIUM)	Magellium/LEGOS (2023b): <a href="https://doi.org/10.24400/527896/A01-2023.012">https://doi.org/10.24400/527896/A01-2023.012</a>	PUM (product user manual): <a href="https://www.aviso.altimetry.fr/fileadmin/documents/data/products/indic/WAMBOR-DT-009-MAG_CopernicusMarine_ServiceEvolution_PUM_v2.0.pdf">https://www.aviso.altimetry.fr/fileadmin/documents/data/products/indic/WAMBOR-DT-009-MAG_CopernicusMarine_ServiceEvolution_PUM_v2.0.pdf</a> *
4	SEALEVEL_GLO_PHY_L4_MY_008_047, L4 reprocessed altimetry observations	EU Copernicus Marine Service Product (2022b)	QUID (quality information document): Pujol et al. (2022) PUM (product user manual): Pujol (2022)

\* Last access: 10 September 2024.

(Greenland and Antarctica) and changes in the global water cycle and land water storage. As such, barystatic sea level changes are a fundamental proxy for climate change and are expected to increase even more dramatically in the future due to increased ice melting, according to future projections (Oppenheimer et al., 2019).

At the regional scale, local dynamics and regional hydrology, together with cross-basin exchanges, modulate regional ocean mass exchanges, called the manometric sea level (Gregory et al., 2019). For instance, Camargo et al. (2022) show that regional trends in the manometric sea level may vary from  $-0.4$  to  $3.3 \text{ mm yr}^{-1}$  across the global ocean for the 2003–2016 period. Typically, regions characterised by high dynamic variability are characterised by large manometric variations. Strong climate modes of variability (e.g. the North Atlantic Oscillation) are also responsible for large deviations in manometric sea level (e.g. Criado-Aldeanueva et al., 2014; Volkov et al., 2019); fingerprinting techniques can be used to estimate the influence of a specific climate index on the resulting sea level variability (e.g. Pfeffer et al., 2022). In the Mediterranean Sea, for instance, variations are intimately linked to the exchanges with the Atlantic Ocean through the Gibraltar Strait and variations in the atmospheric freshwater input, which are both strongly linked to the North Atlantic variability (e.g. Tsimplis and Josey, 2001).

Since 2002, methods to observe and analyse manometric and barystatic sea level variations have generally relied on GRACE (Gravity Recovery And Climate Experiment; e.g. Tapley et al., 2004) and GRACE-FO (GRACE Follow-On; Landerer et al., 2020) satellite mission measurements of the temporal and spatial variations in the Earth's gravity field.

Barystatic and manometric sea level signals can also be inferred from the difference between the total sea level, measured by altimetry missions, and steric sea level, estimated through in situ observations (e.g. Horwath et al., 2022). This approach will be referred to as the sea level budget (SLB) method in the remainder of this article.

Alternatively, ocean general circulation model (OGCM) simulations embed the variability in the sea level and its components, although they significantly lack realism (e.g. Kohl et al., 2007). Ocean reanalyses, which combine an ocean model with observations through data assimilation (Storto et al., 2019b) are in turn able to provide a good estimation of the ocean's long-term changes (e.g. Storto and Yang, 2024) and associated sea level variability at global and basin scales (e.g. Storto et al., 2017); they are thus complementary to gravimetry- and sea-level-budget-based observational counterparts and can be used for several investigations (e.g. Peralta-Ferriz et al., 2014; Marcos, 2015; Hughes et al., 2018). A few limitations in the use of reanalyses exist, though. First, the usual Boussinesq approximation in the OGCMs leads to a zero global steric sea level by construction, as the models cannot represent the global expansion and contraction in the constant volume framework. However, the global steric sea level can be computed and added to the model sea surface height retrospectively, since it does not have any dynamical signature (e.g. Greatbatch, 1994).

There is a more critical and long-standing issue in reanalyses with regard to the barystatic and manometric sea level components. Indeed, both the use of climatological freshwater input from land and ice and the imbalance of the atmospheric freshwater forcing combined with the evapora-

tion and sublimation calculated by the ocean model often make barystatic and manometric terms unrealistic. Some reanalyses correct the barystatic sea level with globally uniform offsets which can be either time-varying or constant. In any case, the barystatic signal is generally unrealistic, and the manometric one may be affected by inaccuracies in the freshwater input into the oceans. In general, ocean-bottom pressure data derived from gravimetry could also be directly assimilated into ocean models (see, e.g., Köhl et al., 2012). However, this approach was found to be suboptimal, mostly due to the low signal-to-noise ratio of the gravimetry data compared to altimetry data assimilation (e.g. Storto et al., 2011) and their issues related to the pre-processing (persistent stripes and land water leakage). More recently, however, ingesting gravimetry data (e.g. in ECCOv4r4; Fukumori et al., 2020) has proven promising to better capture high-frequency sea level variability (Schindelegger et al., 2021). Finally, the limited spatial resolution of the models may limit the representativeness of sea level variations in mesoscale-active areas (e.g. Androsov et al., 2020).

The goal of this paper is manifold. First, we aim to estimate the consistency of the manometric sea level from notably different approaches which use numerical ocean models, gravimetry or altimetry, and in situ observations. These approaches are known to contain different sources of uncertainty, and none of them is fully trustable, as discussed in detail in this section and the next sections. Particular attention is devoted to assessing whether the latest generation of the Copernicus Marine Service global reanalyses can capture the interannual variations in the manometric sea level. Second, we aim at quantifying regional trends and amplitudes to identify the emerging levels and scales of manometric sea level variability, depending on the specific basin. Finally, we aim to fingerprint the manometric sea level with several climate mode indices to connect such variations with large-scale climate variability.

The structure of the paper is as follows: we compare regional (Sect. 3) manometric sea levels from reanalyses with those coming from satellite gravimetry or the sea level budget approach (described in Sect. 2). The exercise will therefore indicate the consistency of the reanalyses and observation-based products for selected metrics. Finally, we summarise the findings and conclude the paper (Sect. 4).

## 2 Data and methods

In this section, we shortly introduce the datasets used in the assessment. We refer to Gregory et al. (2019) for the terminology and definitions used to characterise the sea level components.

### 2.1 Gravimetry-based dataset

Barystatic and manometric sea level anomalies have been estimated from April 2002 to August 2022 at a monthly

timescale and with a spatial resolution of  $1^\circ$ , using an ensemble of GRACE and GRACE-FO solutions (product ref. no. 2 in Table 1). The GRACE and GRACE-FO ensemble is constituted of 120 solutions, allowing us to estimate the uncertainties associated with different processing strategies and geophysical corrections needed for ocean applications. The ensemble is based on coefficients of the Earth's gravitational potential anomalies estimated by five different processing centres (CNES: Centre National d'Etudes Spatiales; CSR: Center for Space Research; JPL: Jet Propulsion Laboratory; GFZ: GeoForschung Zentrum; ITSG: Institute of Geodesy at Graz University of Technology). A large variety of post-processing corrections are applied to the ensemble, including two geocentric motions (Lemoine and Reinquin, 2017; Sun et al., 2016), three oblateness values (C20) of the Earth (Cheng et al., 2013; Lemoine and Reinquin, 2017; Loomis et al., 2019), and two glacial isostatic adjustment (GIA) corrections (Peltier et al., 2015; Caron et al., 2018). To reduce the anisotropic noise characterised by typical stripes elongated in the north–south direction, decorrelation filters, called decorrelation and denoising kernel (DDK) filters (Kusche et al., 2009), are applied to GRACE solutions (e.g. Horvath et al., 2018) using two different orders (DDK3 and DDK6) corresponding to different levels of filtering. The ensemble of 120 solutions results from the combination of these five processing centres, two geocentric models, three oblateness models, two GIA corrections, and two filters. The ensemble standard deviation provides a measure of uncertainty for both the barystatic and manometric sea level time series.

### 2.2 Sea level budget-based dataset

The estimation of barystatic and manometric sea level changes is extended to the altimetry era (January 1993–December 2020) using the sea level budget approach (product ref. no. 3 in Table 1). The manometric sea level changes are calculated as the difference between the geocentric sea level changes based on satellite altimetry and steric sea level changes based on in situ measurements of the seawater temperature and salinity. The reliability of this dataset is intrinsically linked to the altimetry and in situ observational sampling. Only within the global mean values, i.e. the barystatic sea level, are changes computed as the difference between the global mean geocentric sea level changes and thermosteric sea level changes to avoid drifts due to Argo salinity measurement errors (Barnoud et al., 2021; Wong et al., 2020); however, regional (manometric) sea level estimates include the halosteric contribution in the steric evaluation.

Geocentric sea level changes are estimated using the vDT2021 sea level product provided by the Copernicus Climate Change Service (C3S; Legeais et al., 2021). Geocentric sea level changes are corrected for the drifts in the TOPEX-A altimeter (Ablain et al., 2017) and the Jason-3 microwave radiometer wet tropospheric correction (Barnoud et al., 2023a, b) for the GIA effect, using the ensemble mean of 27 GIA

models (Prandi et al., 2021) centred on ICE5G-VM2 (Peltier, 2004), and for the elastic deformation of the solid Earth due to present-day ice melting (Frederikse et al., 2017). The uncertainty in the geocentric sea level changes is calculated with the uncertainty budget and method detailed in Guérou et al. (2023) for the global mean sea level changes and in Prandi et al. (2021) for the local sea level changes. Altimetry data are masked over sea-ice-covered areas using the Copernicus Climate Change Service sea ice product (Lavergne et al., 2019).

Steric sea level changes are estimated as the sum of the thermosteric and halosteric sea level changes calculated from gridded temperature and salinity estimates from three different centres, including EN4 (Good et al., 2013), IAP (Cheng et al., 2020), and Ishii et al. (2006). EN4 provides four datasets with different combinations of corrections for expendable bathythermograph (XBT) and mechanical bathythermograph (MBT) measurements applied, leading to an ensemble of six temperature and salinity datasets. From these datasets, we compute the thermosteric and halosteric sea level changes due to temperature and salinity variations between 0 and 2000 m depth. The deep-ocean contribution (i.e. below 2000 m) is considered only in the global barystatic signal and taken as a linear trend of  $0.12 \pm 0.03 \text{ mm yr}^{-1}$  (Chang et al., 2019) added to the time-varying steric sea level; for the regional estimates of the manometric sea level, the deep-ocean and abyssal-ocean contribution is neglected, as there are not enough data for constraining it at the regional level.

Steric sea level changes are estimated as the ensemble mean of the six solutions, and their uncertainties are estimated with the covariance matrix of the ensemble. The resulting barystatic and manometric uncertainties are described by the covariance matrix obtained by summing the sea level and steric covariance matrices; the sea-ice mask from the altimetry product is propagated onto the resulting manometric product.

### 2.3 The reanalysis dataset

In this work, we use the Global Reanalysis Ensemble Product (GREP) from the Copernicus Marine Service (product ref. no. 1 in Table 1), which is a small-ensemble global reanalysis product, including in turn the four reanalyses of (i) C-GLORS (v7) from CMCC, (ii) GloSea5 from UKMO, (iii) GLORYS2 (V4) from Mercator Ocean, and (iv) ORAS5 from ECMWF. All reanalyses are performed using the NEMO ocean model (Madec and The NEMO System Team, 2017) configured at about  $1/4^\circ$  of the horizontal resolution and 75 levels. However, the four reanalyses differ for several issues, which can be summarised in the (i) NEMO model version and a few selected parameterisations, including the specific choice in the use of the ECMWF reanalysis (ERA-Interim and ERA5) atmospheric forcing; (ii) initial conditions in 1993 at the beginning of the reanalysed period

(1993–2019); (iii) the data assimilation scheme; and (iv) the set of observations assimilated, including their source and pre-processing procedures. Thus, GREP can span, to a good extent, the uncertainty linked with model physics and input datasets. We have used monthly mean data at  $1/4^\circ$  of the horizontal resolution for the comparisons shown in Sect. 3. More details about the four reanalyses, together with some in-situ-based validation and assessment of the ensemble standard deviation, are provided by Storto et al. (2019c).

The estimation approach for GREP follows that of the sea level budget approach (see Sect. 2.2), where the manometric sea level is calculated as the difference in the total sea surface height anomaly from the reanalysis, and the steric sea level anomaly, calculated from the reanalysis output temperature and salinity fields. Thus, we can cross-compare GREP data with GRACE and SLB datasets in terms of the interannual variability, trend, and seasonal amplitude.

### 2.4 Analysis methods

Basin-averaged time series are analysed in the next section as monthly means to assess the main variability signal over three oceanic basins (the Arctic Ocean, defined as the region covering from  $67^\circ \text{N}$  in the Atlantic to the Bering Strait; the North Atlantic Ocean, defined from  $0$  to  $67^\circ \text{N}$ ; the Mediterranean Sea). Time series are also analysed in terms of their interannual and seasonal signal, where the interannual signal is the time series to which the monthly climatology has been subtracted and the seasonal is the residual part, assuming that the majority of the subannual signal can be attributed to seasonal variation, due to the monthly temporal frequency of the data. The uncertainty in the time series corresponds to that provided by the dataset (which in turn uses an ensemble approach to estimate the uncertainty as ensemble standard deviation); by construction, GREP, with only four members, is known to underestimate the uncertainty in the sea level (Storto et al., 2019c). Uncertainty in the trends is estimated through bootstrapping (Efron, 1979) and closely resembles the estimates calculated following Storto et al. (2022). The bootstrapping technique randomly removes part of the time series and thus quantifies the sensitivity of the trend to individual years and periods. Explained variance is used to quantify how much of the regional signal is explained by the global barystatic signal due to fast barotropic motion. For this analysis, we use only global GRACE and SLB time series and show only SLB for the sake of clarity (see, e.g., Barnoud et al., 2023b, for a discussion on their comparison) because the GREP barystatic sea level is either unreliable due to drifts in the freshwater forcing, or it is adjusted to GRACE-derived data and, thus, is not independent. Seasonal amplitude is defined by fitting the monthly data to a curve with sinusoidal (seasonal signal) and linear (trend signal) terms; the interannual variability is the standard deviation of the detrended and deseasonalised time series. Percent values of manometric sea level trends over the total sea level ones are calculated from



the Copernicus Marine Service dataset (product ref. no. 4 in Table 1) over each region.

LASSO regression (Tibshirani, 1997), performed between the normalised manometric sea level and normalised climate indices, is a regularisation technique for multivariate regression, which is used in this study to rank the influence of the climate indices on the basin-averaged manometric sea level in a way similar to what Pfeffer et al. (2022) proposed. Like the previous studies, raw monthly means were used without low-pass filtering the data, which could induce arbitrary preferences in the regression within our multi-variate analysis. After performing a  $k$ -fold cross-validation (with 10 folds) to identify the best hyperparameters, the LASSO regression avoids overfitting the regression, such that absolute values of the regression coefficients quantify the impact of a predictor on the manometric sea level. By construction, LASSO minimises the collinearities across the predictors; however, when predictors are strongly correlated, the preference provided by LASSO might be less obvious than expected (Tibshirani, 1996). We also verified that other methods (e.g. the  $R^2$  hierarchical decomposition from Chevan and Sutherland, 1991) provide the same results. For these analyses, the `glmnet` (Friedman et al., 2010) and `relaimpo` (Groemping, 2006) R packages are used. Finally, for the statistical significance of the correlations and their differences, we used the `psych` R package (Revelle, 2023) that implements Steiger's test for comparing dependent correlations (Steiger, 1980; Olkin and Finn, 1995). All statistical significance results are provided at the 99 % confidence level. The time series and spatial patterns of the climate modes are as in Pfeffer et al. (2022) (see Figs. 1, 3, and 4 therein).

### 3 Results

We present the results of the assessment by first analysing the time series and several diagnostics of the basin-averaged manometric sea level. Then, the consistency between the manometric sea level products is addressed; finally, the influence of the climate modes of variability on the manometric sea level variability is analysed. All results presented refer to the 2003–2019 period that is common to the three datasets.

#### 3.1 Manometric sea level time series

The monthly means of the manometric sea level for the three basins considered in this study is shown in Fig. 1, while several diagnostics (trend, seasonal amplitude, interannual variability, and mean uncertainty, i.e. the time-averaged uncertainty, estimated in turn as the ensemble standard deviation for each product according to Sect. 2) are provided in Table 2 for the three datasets considered.

The three basins (Arctic Ocean, North Atlantic Ocean, and the Mediterranean Sea) exhibit different behaviour; GRACE, SLB, and GREP show, however, that there is qualitatively good consistency in all three seas. The Arctic Ocean has a

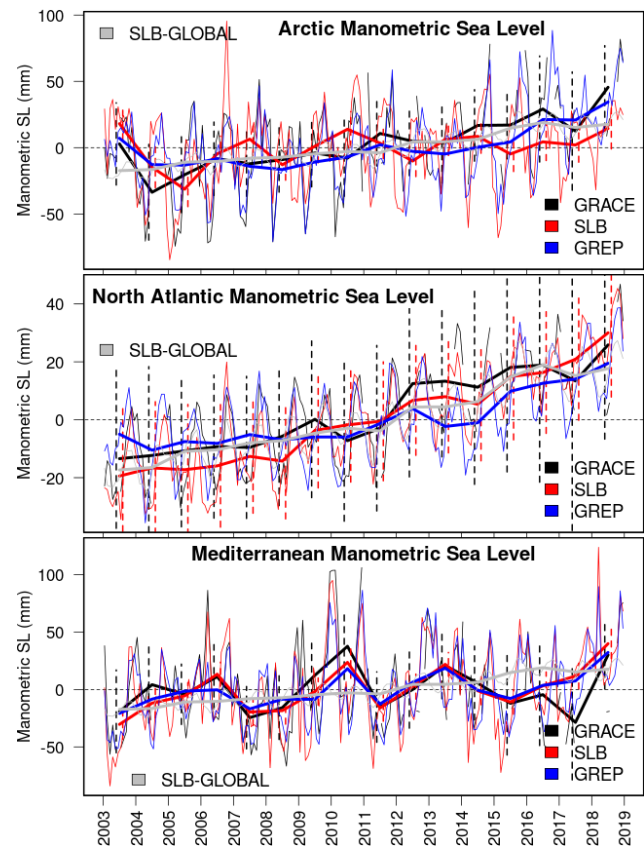


**Figure 1.** Manometric sea level time series for the Arctic, the Mediterranean, and the North Atlantic basins. Both monthly (thin lines) and yearly (thick lines) means are shown for GRACE, SLB, and GREP. The global barystatic sea level (SLB method) is also added in gray. The North Atlantic Ocean is defined from 0 to 67° N, and the Arctic Ocean from 67° N in the Atlantic Ocean to the Bering Strait. Dashed vertical lines correspond to the yearly uncertainty (for GRACE and SLB only; values for GREP are not shown for sake of clarity, given their underestimated value due to the small ensemble size).

regular periodicity and a large seasonal amplitude with a generally increasing yearly mean signal, except during the first years of the time series (2003–2005). For both GRACE and GREP, the latest years are the ones with the largest manometric sea level, which is reflected in large trends found ( $3.45 \pm 0.57$  and  $2.45 \pm 0.44$  mm yr<sup>-1</sup>, respectively) when compared to the other seas, while the SLB shows a weaker trend.

Manometric sea level changes at interannual timescales are very different over the Arctic Ocean than the global ocean (Table 3), meaning that internal dynamics, strait connections, and the sea ice seasonal cycle significantly modulate the regional manometric sea level. Seasonal time series are more largely explained by the global signal for both datasets (38 %–48 %).

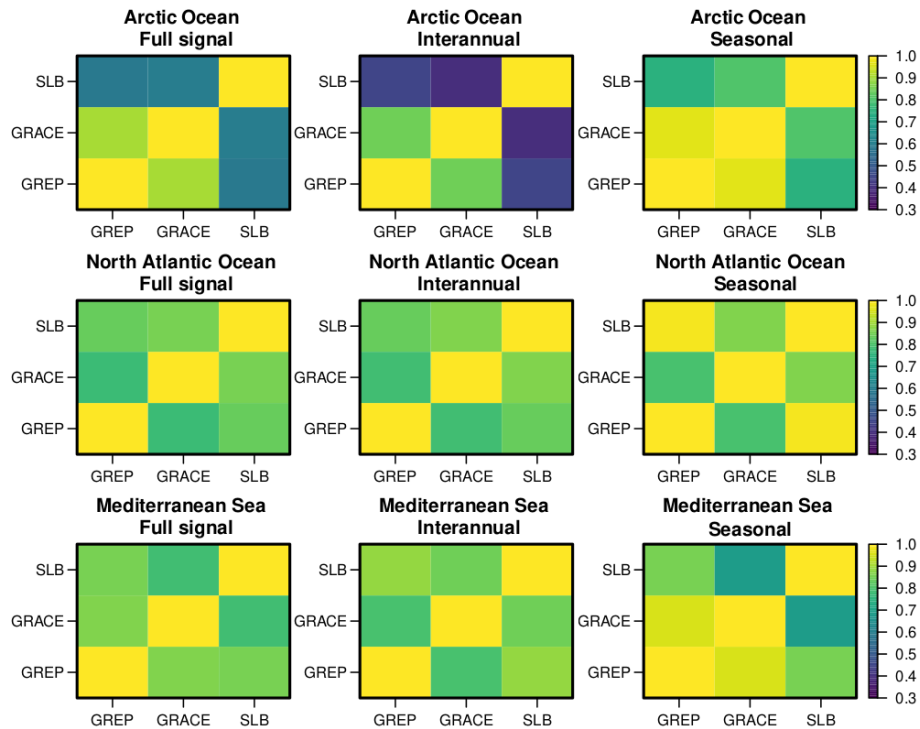


**Figure 2.** Correlation matrix for the three datasets in the three ocean basins investigated in this study, for the full, the interannual, and the seasonal signals. All values of correlation are statistically significant at the 99 % confidence level. Note that the correlation matrix is symmetric, but all terms are shown for the sake of clarity; note also that the minimum correlation in the palette is 0.3, whereas the minimum correlation across all data shown is 0.39.

**Table 2.** Manometric sea level diagnostics for the three basins considered in this study, calculated from the three datasets GREP (ensemble mean), GRACE, and SLB. The trend is calculated as a linear fit, with the uncertainty found through bootstrapping. Seasonal amplitude and interannual variability are defined according to Sect. 2.4. Average uncertainty is calculated from the grid point values. For GREP, it is given by the ensemble standard deviation. Units are given in millimetres per year ( $\text{mm yr}^{-1}$ ) for the trend and millimetres (mm) for the other metrics.

Region	Trend			Seasonal amplitude			Interannual variability			Average uncertainty		
	GRACE	SLB	GREP	GRACE	SLB	GREP	GRACE	SLB	GREP	GRACE	SLB	GREP
Arctic Ocean	$3.45 \pm 0.57$	$1.09 \pm 0.44$	$2.45 \pm 0.44$	29.0	26.0	28.7	20.9	22.2	17.6	29.0	12.9	8.5
North Atlantic Ocean	$2.67 \pm 0.23$	$3.24 \pm 0.16$	$1.81 \pm 0.18$	14.2	10.7	14.4	6.0	6.6	6.1	29.9	20.8	8.0
Mediterranean Sea	$0.87 \pm 0.65$	$2.44 \pm 0.50$	$1.93 \pm 0.46$	31.5	25.5	30.0	27.8	29.2	20.0	31.8	11.8	13.1

The North Atlantic manometric sea level signal has a seasonality (10 to 14 mm, depending on the dataset) that is smaller than the other basins, the smallest interannual variability (6.0 to 6.6 mm), and a nearly linearly increasing mean signal that dominates the variability. The percent variance explained by the global barystatic sea level is large (71 % and 79 % for GRACE and SLB, respectively, for the interannual signal), meaning that the North Atlantic largely resembles the global signal. Here, the manometric trend accounts for about 60 %–80 % of the total sea level trend (provided by altimetry), depending on the specific product used.

In the Mediterranean Sea, the interannual variability is the largest (more than 20 mm for all datasets) and does not follow the global barystatic signal (see the low percent variance

explained in Table 3), especially for the interannual signal, no matter which dataset is considered. This suggests that the regional water cycle and sea level budget are mostly independent of the global one, and this is ascribed to the role of Gibraltar Strait (see, e.g., Landerer and Volkov, 2013). Trends in the Mediterranean Sea are generally lower than in the other basins and explain about 40 %, on average, of the total sea level trend from altimetry. All the datasets exhibit the largest trends in the western part of the Mediterranean Sea (not shown), although with slightly different patterns. Remarkable peaks of the manometric sea level are visible in 2006, 2010, 2011, and 2018; for these events, GREP tends to underestimate the maxima compared to the other two datasets, likely due to the use of climatological discharge

**Table 3.** Percent of the regional manometric sea level variance explained by the global barystatic signal (also for the interannual and seasonal signals). The global barystatic signal is shown in Fig. 1 with gray lines.

Region	Monthly time series		Interannual timescale		Seasonal timescale	
	GRACE	SLB	GRACE	SLB	GRACE	SLB
Arctic Ocean	35 %	11 %	25 %	11 %	48 %	38 %
North Atlantic Ocean	56 %	80 %	71 %	79 %	34 %	85 %
Mediterranean Sea	4 %	19 %	1 %	11 %	8 %	37 %

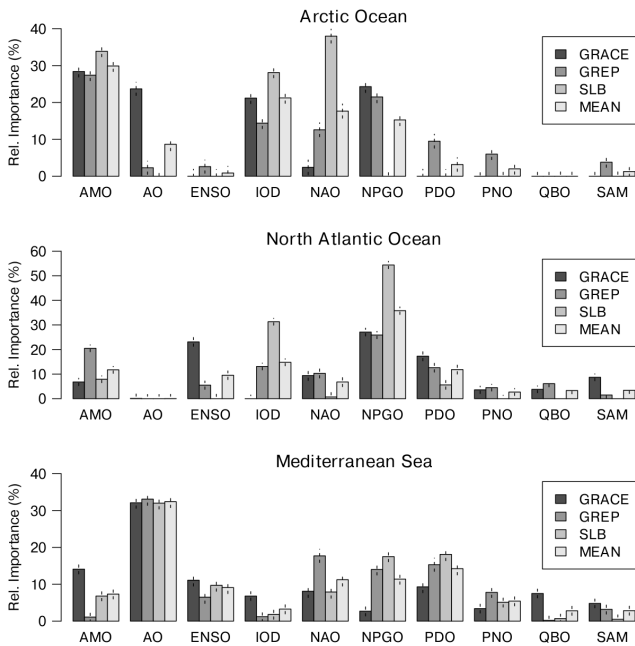


**Figure 3.** Relative importance (defined in Sect. 2.4) of the selected climate indices for the manometric sea level in the three basins investigated in this study, using the three datasets for GRACE, GREP, and SLB. Also shown is the mean of the relative importance over the three datasets (indicated as MEAN). The acronyms for the climate indices are as follows: AMO is for the Atlantic Multidecadal Oscillation; AO is for the Arctic Oscillation; ENSO is for the multivariate El Niño–Southern Oscillation; IOD is for the Indian Ocean Dipole; NAO is for the North Atlantic Oscillation; NPGO is for the North Pacific Gyre Oscillation; PDO is for the Pacific Decadal Oscillation; PNO is for the Pacific North American Oscillation; QBO is for the quasi-biennial oscillation; SAM is for the Southern Annular Mode. Vertical bars indicate the standard errors of the regression coefficients.

from rivers in the reanalyses and the low resolution at Gibraltar Strait affecting the representation of the Mediterranean inflow.

In terms of the uncertainty (see Table 2 and Fig. 1), the GRACE dataset exhibits the largest mean uncertainty (about 30 mm in all basins), while the uncertainty in SLB ranges from about 12 mm in the Arctic Ocean and the Mediterranean Sea to about 21 mm in the North Atlantic Ocean. GREP

uncertainty is the lowest, except in the Mediterranean Sea, where it is comparable to SLB. However, the uncertainty estimates are strongly affected by the ensemble size, which is substantially different across the three datasets (see Sect. 2). Besides, common errors associated, for example, with spatial undersampling, which may be large for the SLB method, will be neglected with the ensemble approach.

### 3.2 Consistency between time series

The consistency between the three time series is investigated by decomposing the full signal into the interannual and seasonal time series. The correlation matrix for the three temporal scales and the three basins is shown in Fig. 2.

In the North Atlantic Ocean and the Mediterranean Sea, the largest correlations are generally between SLB and GREP. SLB and GREP are not independent due to the use of altimetry and in situ observations in both, so this result likely reflects their dependency. At the interannual timescale, the correlation between GRACE and SLB is slightly larger (but the difference is not statistically significant) than that between GRACE and GREP, suggesting that for these regions SLB might capture the year-to-year variations better than the reanalyses. At the seasonal scale in the Mediterranean Sea, however, the consistency between GRACE and GREP is larger than that between GRACE and SLB (with a statistically significant difference), suggesting that the reanalyses capture the seasonal cycle better than SLB with respect to gravimetry data. For both regions, the high consistency of manometric sea level from reanalyses compared to the two observation-based datasets suggests the good reliability of the GREP ensemble mean in capturing the sea level variations.

In the Arctic Ocean, a large consistency is found between GRACE and GREP; the correlations involving SLB are statistically significantly lower than the others at all timescales (full, interannual, and seasonal) at the 99 % confidence level; this is also visible in Fig. 1, as fluctuations in the SLB time series are not reproduced by the other two datasets. On the one hand, the meridional transports, sea ice modelling, and atmospheric forcing that are implicit in the reanalysis systems are known to be able to shape the Arctic Ocean interannual variability realistically (see, e.g., Mayer et al., 2016, 2019); on the other hand, altimetry and in situ data are poorly

sampled in the Arctic Ocean, making it more challenging to apply the SLB approach therein. By separating the total sea level and the steric sea level contributions for the SLB and GREP methods (not shown), we have found good consistency for the total sea level interannual signal (correlation coefficient equal to 0.69) compared to the steric component (0.35); this suggests that the SLB method has problems over the Arctic basin with respect to representing steric sea level variations, possibly due to the poor in situ observational sampling.

### 3.3 Influence of climate indices on manometric sea level variations

Several climate indices are considered predictors for the manometric sea level in the three basins (Arctic Ocean, North Atlantic Ocean, and the Mediterranean Sea). Their acronyms and meanings are listed in the caption of Fig. 3. The detailed justification for inclusion in the analysis is provided by Han et al. (2017), Cazenave and Moreira (2022), and Pfeffer et al. (2022), among many others. Through representing well-determined atmospheric circulation regimes and internal climate variability, the indices synthesise the water cycle and the atmospheric forcing variability regimes, leading in turn to variations in the regional manometric sea level due to changes in oceanic divergence and freshwater forcing. For instance, the El Niño–Southern Oscillation (ENSO) has a prominent role in modifying precipitation patterns, with obvious implications for the manometric sea level (e.g. Muis et al., 2018); changes in the North Atlantic Oscillation (NAO) modify atmospheric and oceanic transport in North America and Europe, also implying changes in the Mediterranean Sea through modifications and exchanges at Gibraltar and precipitation patterns (Landerer et al., 2013; Storto et al., 2019a). It is beyond the scope of this study to explain all of the possible modes of co-variability, and the interested readers are referred to the specific literature for a broad overview (e.g. Andrew et al., 2006; Peralta-Ferriz et al., 2014; Merrifield and Thompson, 2018; Volkov et al., 2019; Pfeffer et al., 2022). Raw monthly means of the manometric sea level are used in this study to avoid arbitrary filtering affecting the regression results; the climate indices, however, are used with filtering (as in their standard definition).

In the Arctic Ocean, the largest influence is found to be due to the Atlantic Multidecadal Oscillation (AMO), with values ranging from 25 % to 35 %, depending on the dataset. AMO is known to modulate the sea ice interannual variations and the Arctic amplification (Li et al., 2018; Fang et al., 2022), which are both important contributors to the sea level manometric fluctuations, due to the increased melting of land ice and disturbances in atmospheric and ocean circulation that jointly influence the variability in manometric sea levels (see, e.g., Previdi et al., 2021). The IOD (Indian Ocean Dipole), NAO, and NPGO (North Pacific Gyre Oscillation) also significantly affect the Arctic manometric sea level, although

the consensus between the datasets varies, and the influence of the IOD is questionable. The Arctic Oscillation is found to be influential when using the GRACE dataset consistently with previous studies (Peralta-Ferriz et al., 2014), although the other datasets show, in general, other preferences.

The North Atlantic manometric sea level is characterised by the largest impact of NPGO, and this is consistent across all of the datasets. While NPGO explains the variations in the eastern North Pacific Ocean well (Di Lorenzo et al., 2008), its impact on the North Atlantic manometric sea level likely depends on its global- and large-scale influence (Iglesias et al., 2017; Litzow et al., 2020; Pfeffer et al., 2022), which in turn drives, to a large extent, the North Atlantic manometric sea level variability (see Table 3). NPGO accounts for more than 25 % of the North Atlantic manometric sea level variability, peaking at more than 40 % for the SLB dataset. A significant impact in the North Atlantic manometric sea level is also given by variations described by the PDO (Pacific Decadal Oscillation), AMO, and IOD, although for the latter there is a small consistency found across the datasets.

Finally, in the Mediterranean Sea, the largest influence is provided by the Arctic Oscillation (AO), which explains more than 30 % of the manometric sea level covariations for all datasets. AO is an expression of the North Atlantic variability, strictly linked to the NAO and closely linked to the northern European wind circulation (e.g. Ambaum et al., 2001); while these are strictly connected, the regularisation technique used here clearly indicates that AO is a better predictor than NAO for the regional manometric sea level; however, this might be an artefact of the LASSO minimisation that chooses only one among strongly correlated predictors. Other influential climate modes of variability in the Mediterranean Sea are linked to the North Pacific variability, namely the PDO and NPGO, likely due to their effect on the North Atlantic variability.

## 4 Summary and discussion

In this study, we have focused on the basin-averaged manometric sea level for a few regional basins (Arctic Ocean, North Atlantic Ocean, and the Mediterranean Sea) and from different datasets to investigate the consistency, the emerging climate signals, the differences between the basin characteristics, and the link with the main large-scale modes of variability. These three basins were chosen as part of the focus of the EU Copernicus Marine Service and are large enough to be resolved at the basin scale by the observational and modelling systems used herein, unlike other smaller basins.

To the authors' knowledge, this is the first time that different datasets of manometric sea level from reanalyses, gravimetry, and altimetry (minus in situ data) are compared at the regional level to infer their strengths and weaknesses. The three basins (Arctic Ocean, North Atlantic Ocean, and the Mediterranean Sea) exhibit inherently different features,



with the Mediterranean Sea showing, on average over the three products, the largest interannual variability and the smallest trends; the Arctic Ocean shows a large seasonal amplitude and the largest trend, and the North Atlantic Ocean shows a quasi-linear trend, which is very well explained by the global barystatic signal. The three products are found to be in reasonable agreement, with all pairs significantly correlated at both interannual and seasonal timescales. There are, however, non-negligible differences in the quantitative assessment; for instance, GRACE leads to a large trend in the Arctic basin ( $3.45 \pm 0.57 \text{ mm yr}^{-1}$ ) which is not reproduced by either GREP or SLB and needs to be investigated in more detail. There is also a trend in the Mediterranean Sea that is smaller than the others.

In the Arctic Ocean, the altimetry minus in situ (SLB) information is generally in less agreement with the other datasets based on correlation scores; this seems to be due to the poor in situ observation sampling on which the SLB approach is based (see the product user manual, PUM; Table 1), which could be alleviated in reanalyses, to some extent, by the atmospheric forcing information and the meridional exchanges. In the Mediterranean Sea, seasonal-scale agreement is also the largest between GRACE and GREP, suggesting in turn that the Copernicus Marine Service global reanalyses can capture the manometric sea level variability in the studied regions.

Finally, a fingerprinting technique based on a regularisation in the regression is used to quantify the influence of several large-scale climate modes of variability in the basin-averaged manometric sea level. In most cases, we found consistency in the results using the three different datasets. The analysis indicates the NPGO (North Pacific Gyre Oscillation), AO (Arctic Oscillation), and AMO (Atlantic Multidecadal Oscillation) to be the most influential modes for the North Atlantic Ocean, the Mediterranean Sea, and the Arctic Ocean, respectively. This is the combined result of the barystatic sea level signature, cross-basin exchanges, and teleconnection patterns, as explained in detail in previous studies (Landerer and Volkov, 2013; Iglesias et al., 2017; Fang et al., 2022). These results are useful as a reference for further fingerprinting technique applications and as a possible tool for statistical prediction of manometric variations.

The results provide a summary of the manometric sea level variability within the three basins investigated here and guide users with respect to the choice of the specific product, depending on the region of interest. The overarching conclusions are that reanalyses, when an ensemble mean of different systems is adopted, provide good performances in all basins; SLB performance is the most affected by observational sampling and thus should be avoided in regions with poorly developed networks; and gravimetry data provide realistic sub-seasonal and interannual variability, although long-term trends are less consistent than other datasets, and the monthly uncertainty is the largest.

Further studies are needed to understand the different behaviour of the datasets for certain aspects (e.g. the overestimation of the Arctic Ocean manometric sea level trend by GRACE or its underestimation in the Mediterranean Sea), namely whether this is due to some intrinsic limitation of the data processing or the different processes implied by the measurement techniques.

**Data availability.** See Table 1 to access the data through the associated DOIs.

**Author contributions.** AS designed the analysis and wrote most of the text. GC and AS performed the analysis. JP coordinated the processing of the manometric sea level data from GRACE, revised the paper, and provided many comments on the use of the observation-based datasets and the fingerprinting technique. AB corrected the detail in Sect. 2. All authors contributed with data production and suggestions for improving the study.

**Competing interests.** The contact author has declared that none of the authors has any competing interests.

**Disclaimer.** The Copernicus Marine Service offering is regularly updated to ensure it remains at the forefront of user requirements. In this process, some products may undergo replacement or renaming, leading to the removal of certain product IDs from our catalogue. If you have any questions or require assistance regarding these modifications, please feel free to reach out to our user support team for further guidance. They will be able to provide you with the necessary information to address your concerns and find suitable alternatives, maintaining our commitment to delivering top-quality services.

Publisher's note: Copernicus Publications remains neutral with regard to jurisdictional claims made in the text, published maps, institutional affiliations, or any other geographical representation in this paper. While Copernicus Publications makes every effort to include appropriate place names, the final responsibility lies with the authors.

**Acknowledgements.** The authors thank the OSR8 team (Karina von Schuckmann and Lorena Moreira Mendez) for their coordination efforts and suggestions to improve the quality of the original version of the paper.

**Financial support.** This work has been supported by the GLORAN-Lot8 and the WAMBOR contracts of the Copernicus Marine Service.

**Review statement.** This paper was edited by Marta Marcos and reviewed by Don Chambers and two anonymous referees.

## References

- Ablain, M., Legeais, J. F., Prandi, P., Marcos, M., Fenoglio-Marc, L., Dieng, H. B., Benveniste, J., and Cazenave, A.: Satellite altimetry-based sea level at global and regional scales, *Surv. Geophys.*, 38, 7–31, 2017.
- Ambaum, M. H. P., Hoskins, B. J., and Stephenson, D. B.: Arctic Oscillation or North Atlantic Oscillation?, *J. Climate*, 14, 3495–3507, [https://doi.org/10.1175/1520-0442\(2001\)014<3495:AONAO>2.0.CO;2](https://doi.org/10.1175/1520-0442(2001)014<3495:AONAO>2.0.CO;2), 2001.
- Amin, H., Bagherbandi, M., and Sjöberg, L. E.: Quantifying barystatic sea-level change from satellite altimetry, GRACE and Argo observations over 2005–2016, *Adv. Space Res.*, 65, 1922–1940, 2020.
- Andrew, J. A. M., Leach, H., and Woodworth, P. L.: The relationships between tropical Atlantic sea level variability and major climate indices, *Ocean Dynam.*, 56, 452–463, <https://doi.org/10.1007/s10236-006-0068-z>, 2006.
- Androsov, A., Boebel, O., Schröter, J., Danilov, S., Macrandar, A., and Ivanciu, I.: Ocean bottom pressure variability: Can it be reliably modeled? *J. Geophys. Res.-Oceans*, 125, e2019JC015469, <https://doi.org/10.1029/2019JC015469>, 2020.
- Barnoud, A., Pfeffer, J., Guérou, A., Frery, M.-L., Siméon, M., Cazenave, A., Chen, J., Llovel, W., Thierry, V., Legéais, J.-F., and Ablain, M.: Contributions of altimetry and Argo to non-closure of the global mean sea level budget since 2016, *Geophys. Res. Lett.*, 48, e2021GL092824, <https://doi.org/10.1029/2021gl092824>, 2021.
- Barnoud, A., Picard, B., Meyssignac, B., Marti, F., Ablain, M., and Roca, R.: Reducing the uncertainty in the satellite altimetry estimates of global mean sea level trends using highly stable water vapor climate data records, *J. Geophys. Res.-Oceans*, 128, e2022JC019378, <https://doi.org/10.1029/2022JC019378>, 2023a.
- Barnoud, A., Pfeffer, J., Cazenave, A., Fraudeau, R., Rousseau, V., and Ablain, M.: Revisiting the global mean ocean mass budget over 2005–2020, *Ocean Sci.*, 19, 321–334, <https://doi.org/10.5194/os-19-321-2023>, 2023b.
- Camargo, C. M. L., Riva, R. E. M., Hermans, T. H. J., and Slangen, A. B. A.: Trends and uncertainties of mass-driven sea-level change in the satellite altimetry era, *Earth Syst. Dynam.*, 13, 1351–1375, <https://doi.org/10.5194/esd-13-1351-2022>, 2022.
- Caron, L., Ivins, E., Larour, E., Adhikari, S., Nilsson, J., and Blewitt, G.: GIA model statistics for GRACE hydrology, cryosphere, and ocean science, *Geophys. Res. Lett.*, 45, 2203–2212, 2018.
- Cazenave, A., and Moreira, L.: Contemporary sea-level changes from global to local scales: a review, *P. Math. Phys. Eng. Sci.*, 25, 478, 20220049, <https://doi.org/10.1098/rspa.2022.0049>, 2022.
- Chang, L., Tang, H., Wang, Q., and Sun, W.: Global thermosteric sea level change contributed by the deep ocean below 2000 m estimated by Argo and CTD data, *Earth Planet. Sc. Lett.*, 524, 115727, <https://doi.org/10.1016/j.epsl.2019.115727>, 2019.
- Cheng, M., Tapley, B. D., and Ries, J. C.: Deceleration in the Earth's oblateness, *J. Geophys. Res.*, 118, 740–747, <https://doi.org/10.1002/jgrb.50058>, 2013.
- Criado-Aldeanueva, F., Soto-Navarro, F. J., and García-Lafuente, J.: Large-scale atmospheric forcing influencing the long-term variability of Mediterranean heat and freshwater budgets: Climatic indices, *J. Hydrometeorol.*, 15, 650–663, 2014.
- Cheng, L., Trenberth, K. E., Gruber, N., Abraham, J. P., Fasullo, J. T., Li, G., Mann, M. E., Zhao, X., and Zhu, J.: Improved Estimates of Changes in Upper Ocean Salinity and the Hydrological Cycle, *J. Climate*, 33, 10357–10381, <https://doi.org/10.1175/JCLI-D-20-0366.1>, 2020.
- Chevan, A. and Sutherland, M.: Hierarchical Partitioning, *Am. Stat.* 45, 90–96, 1991.
- Desportes, C., Garric, G., Régnier, C., Drévilion, M., Parent, L., Drilllet, Y., Masina, S., Storto, A., Mirouze, I., Cipollone, A., Zuo, H., Balmaseda, M., Peterson, D., Wood, R., Jackson, L., Mulet, S., Grenier, E., and Gounou, A.: EU Copernicus Marine Service Quality Information Document for the Global Ocean Ensemble Physics Reanalysis, GLOBAL\_REANALYSIS\_PHY\_001\_031, Issue 1.1, Mercator Ocean International, <https://catalogue.marine.copernicus.eu/documents/QUID/CMEMS-GLO-QUID-001-031.pdf> (last access: 24 July 2023), 2022.
- Di Lorenzo, E., Schneider, N., Cobb, K. M., Franks, P. J. S., Chhak, K., Miller, A. J., McWilliams, J. C., Bograd, S. J., Arango, H., Curchitser, E., Powell, T. M., and Rivière, P.: North Pacific Gyre Oscillation links ocean climate and ecosystem change, *Geophys. Res. Lett.*, 35, L08607, <https://doi.org/10.1029/2007GL032838>, 2008.
- Efron, B.: Bootstrap methods: Another look at the jackknife, *Ann. Stat.*, 7, 1–26, <https://doi.org/10.1214/aos/1176344552>, 1979.
- EU Copernicus Marine Service Product: Global Ocean Ensemble Physics Reanalysis, Mercator Ocean International [data set], <https://doi.org/10.48670/moi-00024>, 2022a.
- EU Copernicus Marine Service Product: Global Ocean Gridded L 4 Sea Surface Heights And Derived Variables Reprocessed 1993 Ongoing, Mercator Ocean International [data set], <https://doi.org/10.48670/moi-00148>, 2022b.
- Fang, M., Li, X., Chen, H. W., and Chen, D.: Arctic amplification modulated by Atlantic Multidecadal Oscillation and greenhouse forcing on multidecadal to century scales, *Nat. Commun.*, 13, 1865, <https://doi.org/10.1038/s41467-022-29523-x>, 2022.
- Fox-Kemper, B., Hewitt, H. T., Xiao, C., Aðalgeirsdóttir, G., Drijfhout, S. S., Edwards, T. L., N. R. Golledge, M. H., Kopp, R. E., Krinner, G., Mix, A., Notz, D., Nowicki, S., Nurhati, I. S., Ruiz, L., Sallée, J.-B., Slangen, A. B. A., and Yu, Y.: Ocean, Cryosphere and Sea Level Change, in: *Climate Change 2021: The Physical Science Basis. Contribution of Working Group I to the Sixth Assessment Report of the Intergovernmental Panel on Climate Change*, edited by: Masson-Delmotte, V., Zhai, P., Pirani, A., Connors, S. L., Péan, C., Berger, S., Caud, N., Chen, Y., Goldfarb, L., Gomis, M. I., Huang, M., Leitzell, K., Lonnoy, E., Matthews, J. B. R., Maycock, T. K., Waterfield, T., Yelekçi, O., Yu, R., and Zhou B., Cambridge University Press, Cambridge, United Kingdom and New York, NY, USA, 1211–1362, <https://doi.org/10.1017/9781009157896.011>, 2021.
- Frederikse, T., Riva, R. E. M., and King, M. A.: Ocean bottom deformation due to present-day mass redistribution and its impact on sea level observations, *Geophys. Res. Lett.*, 44, 12306–12314, <https://doi.org/10.1002/2017GL075419>, 2017.
- Frederikse, T., Landerer, F., Caron, L., Adhikari, S., Parkes, D., Humphrey, V. W., Dangendorf, S., Hogarth, P., Zanna, L., Cheng, L., and Wu, Y. H.: The causes of sea-level rise since 1900, *Nature*, 584, 393–397, <https://doi.org/10.1038/s41586-020-2591-3>, 2020.

- Friedman, J. H., Hastie, T., and Tibshirani, R.: Regularization Paths for Generalized Linear Models via Coordinate Descent, *J. Stat. Softw.*, 33, 1–22, <https://doi.org/10.18637/jss.v033.i01>, 2010.
- Fukumori, I., Wang, O., Fenty, I., Forget, G., Heimbach, P., Ponte, R. M.: ECCO Version 4 Release 4, [https://ecco-group.org/docs/v4r4\\_synopsis.pdf](https://ecco-group.org/docs/v4r4_synopsis.pdf), last access: 7 August 2020.
- Good, S. A., Martin, M. J., and Rayner, N. A.: EN4: quality controlled ocean temperature and salinity profiles and monthly objective analyses with uncertainty estimates, *J. Geophys. Res.-Oceans*, 118, 6704–6716, <https://doi.org/10.1002/2013JC009067>, 2013.
- Gounou, A., Drevillon, M., and Clavier, M.: EU Copernicus Marine Service Product User Manual for the Global Ocean Ensemble Physics Reanalysis, GLOBAL\_REANALYSIS\_PHY\_001\_031, Issue 1.1, Mercator Ocean International, <https://catalogue.marine.copernicus.eu/documents/PUM/CMEMS-GLO-PUM-001-031.pdf> (last access: 24 July 2023), 2022.
- Greatbatch, R. J.: A note on the representation of steric sea level in models that conserve volume rather than mass, *J. Geophys. Res.*, 99, 12767–12771, <https://doi.org/10.1029/94JC00847>, 1994.
- Gregory, J. M., Griffies, S. M., Hughes, C. W., Lowe, J. A., Church, J. A., Fukumori, I., Gomez, N., Kopp, R. E., Landerer, F., Cozannet, G. L., Ponte, R. M., Stammer, D., Tamisiea, M. E., and van de Wal, R. S.: Concepts and Terminology for Sea Level: Mean, Variability and Change, Both Local and Global, *Surv. Geophys.*, 40, 1251–1289, <https://doi.org/10.1007/s10712-019-09525-z>, 2019.
- Groemping, U.: Relative Importance for Linear Regression in R: The Package relaimpo, *J. Stat. Softw.*, 17, 1–27, <https://doi.org/10.18637/jss.v017.i01>, 2006.
- Guérou, A., Meyssignac, B., Prandi, P., Ablain, M., Ribes, A., and Bignalet-Cazalet, F.: Current observed global mean sea level rise and acceleration estimated from satellite altimetry and the associated measurement uncertainty, *Ocean Sci.*, 19, 431–451, <https://doi.org/10.5194/os-19-431-2023>, 2023.
- Han, W., Meehl, G. A., Stammer, D., Hu, A., Hamlington, B., Kenigson, J., Palanisamy, H., and Thompson, P.: Spatial Patterns of Sea Level Variability Associated with Natural Internal Climate Modes, *Surv. Geophys.*, 38, 217–250, <https://doi.org/10.1007/s10712-016-9386-y>, 2017.
- Horvath, A., Murböck, M., Pail, R., and Horvath, M.: Decorrelation of GRACE time variable gravity field solutions using full covariance information, *Geosciences*, 8, 323, <https://doi.org/10.3390/geosciences8090323>, 2018.
- Horvath, M., Gutknecht, B. D., Cazenave, A., Palanisamy, H. K., Marti, F., Marzeion, B., Paul, F., Le Bris, R., Hogg, A. E., Otsaka, I., Shepherd, A., Döll, P., Cáceres, D., Müller Schmied, H., Johannessen, J. A., Nilsen, J. E. Ø., Raj, R. P., Forsberg, R., Sandberg Sørensen, L., Barletta, V. R., Simonsen, S. B., Knudsen, P., Andersen, O. B., Rannald, H., Rose, S. K., Merchant, C. J., Macintosh, C. R., von Schuckmann, K., Novotny, K., Groh, A., Restano, M., and Benveniste, J.: Global sea-level budget and ocean-mass budget, with a focus on advanced data products and uncertainty characterisation, *Earth Syst. Sci. Data*, 14, 411–447, <https://doi.org/10.5194/essd-14-411-2022>, 2022.
- Hughes, C. W., Williams, J., Blaker, A., Coward, A., and Stepanov, V.: A window on the deep ocean: The special value of ocean bottom pressure for monitoring the large-scale, deep-ocean circulation, *Prog. Oceanogr.*, 161, 19–46, <https://doi.org/10.1016/j.pocean.2018.01.011>, 2018.
- Iglesias, I., Lorenzo, M. N., Lázaro, C., Fernandes, M. J., and Santos, L.: Sea level anomaly in the North Atlantic and seas around Europe: Long-term variability and response to North Atlantic teleconnection patterns, *Sci. Total Environ.*, 609, 861–874, 2017.
- Ishii, M., Kimoto, M., Sakamoto, K., and Iwasaki, S. I.: Steric sea level changes estimated from historical ocean subsurface temperature and salinity analyses, *J. Oceanogr.*, 62, 155–170, 2006.
- Köhl, A., Stammer, D., and Cornuelle, B.: Interannual to Decadal Changes in the ECCO Global Synthesis, *J. Phys. Oceanogr.*, 37, 313–337, 2007.
- Köhl, A., Siegmund, F., and Stammer, D.: Impact of assimilating bottom pressure anomalies from GRACE on ocean circulation estimates, *J. Geophys. Res.*, 117, C04032, <https://doi.org/10.1029/2011JC007623>, 2012.
- Kusche, J., Schmidt, R., Petrovic, S., and Rietbroek, R.: Decorrelated GRACE time-variable gravity solutions by GFZ, and their validation using a hydrological model, *J. Geodesy*, 83, 903–913, <https://doi.org/10.1007/s00190-009-0308-3>, 2009.
- Landerer, F. W. and Volkov, D. L.: The anatomy of recent large sea level fluctuations in the Mediterranean Sea, *Geophys. Res. Lett.*, 40, 553–557, <https://doi.org/10.1002/grl.50140>, 2013.
- Landerer, F. W., Flechtner, F. M., Save, H., Webb, F. H., Bandikova, T., Bertiger, W. I., Bettadpur, S. V., Byun, S. H., Dahle, C., Döbbslaw, H., and Fahnstock, E.: Extending the global mass change data record: GRACE Follow-On instrument and science data performance, *Geophys. Res. Lett.*, 47, e2020GL088306, <https://doi.org/10.1029/2020GL088306>, 2020.
- Lavergne, T., Sørensen, A. M., Kern, S., Tonboe, R., Notz, D., Aaboe, S., Bell, L., Dybkjær, G., Eastwood, S., Gabarro, C., Heygster, G., Killie, M. A., Brandt Kreiner, M., Lavelle, J., Saldo, R., Sandven, S., and Pedersen, L. T.: Version 2 of the EUMETSAT OSI SAF and ESA CCI sea-ice concentration climate data records, *The Cryosphere*, 13, 49–78, <https://doi.org/10.5194/tc-13-49-2019>, 2019.
- Legeais, J.-F., Meyssignac, B., Faugère, Y., Guérou, A., Ablain, M., Pujol, M.-I., Dufau, C., and Dibarboure G.: Copernicus Sea Level Space Observations: A Basis for Assessing Mitigation and Developing Adaptation Strategies to Sea Level Rise, *Front. Mar. Sci.*, 8, 704721, <https://doi.org/10.3389/fmars.2021.704721>, 2021.
- Lemoine, J.-M. and Requin, F.: Processing of SLR Observations at CNES, Newsletter EGSIM, 3 pp., [http://www.egsim.eu/images/Newsletters/EGSIM\\_newsletter\\_no10.pdf](http://www.egsim.eu/images/Newsletters/EGSIM_newsletter_no10.pdf) (last access: 10 September 2024), 2017.
- Li, F., Orsolini, Y. J., Wang, H., Gao, Y., and He, S.: Atlantic multidecadal oscillation modulates the impacts of Arctic sea ice decline, *Geophys. Res. Lett.*, 45, 2497–2506, <https://doi.org/10.1002/2017GL076210>, 2018.
- Litzow, M. A., Malick, M. J., Bond, N. A., Cunningham, C. J., Gosselin, J. L., and Ward, E. J.: Quantifying a novel climate through changes in PDO-climate and PDO-salmon relationships, *Geophys. Res. Lett.*, 47, e2020GL087972, <https://doi.org/10.1029/2020GL087972>, 2020.
- Loomis, B. D., Rachlin, K. E., and Luthcke, S. B.: Improved Earth oblateness rate reveals increased ice sheet losses and mass-driven sea level rise, *Geophys. Res. Lett.*, 46, 6910–6917, <https://doi.org/10.1029/2019GL082929>, 2019.

- Madec G. and The NEMO System Team: NEMO ocean engine, note Du pole de modélisation (Paris, France: Institut Pierre-Simon Laplace), Zenodo [code], <https://doi.org/10.5281/zenodo.3248739>, 2017.
- Magellium/LEGOS: Barystatic and manometric sea level changes from GRACE and GRACE-FO (Version 4) [NetCDF], CNES [data set], <https://doi.org/10.24400/527896/A01-2023.011,2023a>.
- Magellium/LEGOS: Barystatic and manometric sea level changes from a sea level budget approach (Version 2) [NetCDF], CNES [data set], <https://doi.org/10.24400/527896/A01-2023.012,2023b>.
- Marcos, M.: Ocean bottom pressure variability in the Mediterranean Sea and its relationship with sea level from a numerical mode, *Global Planet. Change*, 124, 10–21, 2015.
- Mayer, M., Haimberger, L., Pietschnig, M., and Storto, A.: Facets of Arctic energy accumulation based on observations and reanalyses 2000–2015, *Geophys. Res. Lett.*, 43, 10420–10429, <https://doi.org/10.1002/2016GL070557>, 2016.
- Mayer, M., Tietsche, S., Haimberger, L., Tsubouchi, T., Mayer, J., and Zuo, H.: An Improved Estimate of the Coupled Arctic Energy Budget, *J. Climate*, 32, 7915–7934, <https://doi.org/10.1175/JCLI-D-19-0233.1>, 2019.
- Merrifield, M. A. and Thompson, P. R.: Interdecadal sea level variations in the Pacific: Distinctions between the tropics and extratropics, *Geophys. Res. Lett.*, 45, 6604–6610, 2018.
- Muis, S., Haigh, I. D., Guimarães Nobre, G., Aerts, J. C. J. H., and Ward, P. J.: Influence of El Niño-Southern Oscillation on global coastal flooding, *Earth's Future*, 6, 1311–1322, <https://doi.org/10.1029/2018EF000909>, 2018.
- Olkin, I. and Finn, J. D.: Correlations redux, *Psychol. Bull.*, 118, 155–164, <https://doi.org/10.1037/0033-2909.118.1.155>, 1995.
- Oppenheimer, M., Abdelgawad, A., Hay, J., Glavovic, B., Cai, R., Marzeion, B., Hinkel, J., Cifuentes-Jara, M., Meyssignac, B., Van De Wal, R., DeConto, R., Sebesvari, Z., Magnan, A., and Ghosh, Hay, T. J., Isla, F., Marzeion, B., Meyssignac, B., and Sebesvari, Z.: Sea Level Rise and Implications for Low-Lying Islands, Coasts and Communities, in: IPCC Special Report on the Ocean and Cryosphere in a Changing Climate, edited by: Pörtner, H.-O., Roberts, D. C., Masson-Delmotte, V., Zhai, P., Tignor, M., Poloczanska, E., Mintenbeck, K., Alegría, A., Nicolai, M., Okem, A., Petzold, J., Rama, B., Weyer, N. M., Cambridge University Press, Cambridge, UK and New York, NY, USA, 321–445, <https://doi.org/10.1017/9781009157964.006>, 2019.
- Peltier, W. R.: Global Glacial Isostasy and the Surface of the Ice-Age Earth: The ICE-5G (VM2) Model and GRACE, *Annu. Rev. Earth Pl. Sc.*, 32, 111–149, 2004.
- Peltier, W. R., Argus, D. F., and Drummond, R.: Space geodesy constrains ice age terminal deglaciation: the global ICE-6G (VM5a) model, *J. Geophys. Res.*, 120, 450–487, 2015.
- Peralta-Ferriz, C., Morison, J. H., Wallace, J. M., Bonin, J. A., and Zhang, J.: Arctic Ocean Circulation Patterns Revealed by GRACE, *J. Climate*, 27, 1445–1468, <https://doi.org/10.1175/JCLI-D-13-00013.1>, 2014.
- Pfeffer, J., Cazenave, A., and Barnoud, A.: Analysis of the interannual variability in satellite gravity solutions: detection of climate modes fingerprints in water mass displacements across continents and oceans, *Clim. Dynam.*, 58, 1065–1084, <https://doi.org/10.1007/s00382-021-05953-z>, 2022.
- Prandi, P., Meyssignac, B., Ablain, M., Spada, G., Ribes, A., and Benveniste, J.: Local sea level trends, accelerations and uncertainties over 1993–2019, *Sci. Data*, 8, 1, <https://doi.org/10.1038/s41597-020-00786-7>, 2021.
- Previdi, M., Smith, K. L., and Polvani, L. M.: Arctic amplification of climate change: a review of underlying mechanisms, *Environ. Res. Lett.*, 16, 093003, <https://doi.org/10.1088/1748-9326/ac1c29>, 2021.
- Pujol, M.-I.: EU Copernicus Marine Service Product User Manual for the For Sea Level Altimeter products, Issue 7.0, Mercator Ocean International, <https://catalogue.marine.copernicus.eu/documents/PUM/CMEMS-SL-PUM-008-032-068.pdf> (last access: 24 July 2023), 2022.
- Pujol, M.-I., Taburet, G., and SL-TAC team: EU Copernicus Marine Service Quality Information Document for the Sea Level TAC – DUACS products, Issue 8.2, Mercator Ocean International, <https://catalogue.marine.copernicus.eu/documents/QUID/CMEMS-SL-QUID-008-032-068.pdf> (last access: 24 July 2023), 2022.
- Revelle, W.: Psych: Procedures for Psychological, Psychometric, and Personality Research, R package version 2.3.6, Northwestern University, Evanston, Illinois [code], <https://CRAN.R-project.org/package=psych> (last access: 27 June 2024), 2023.
- Schindelegger, M., Harker, A. A., Ponte, R. M., Dobslaw, H., and Salstein, D. A.: Convergence of daily GRACE solutions and models of submonthly ocean bottom pressure variability, *J. Geophys. Res.-Oceans*, 126, e2020JC017031, <https://doi.org/10.1029/2020JC017031>, 2021.
- Steiger, J. H.: Tests for comparing elements of a correlation matrix, *Psychol. Bull.*, 87, 245–251, 1980.
- Storto, A. and Yang, C.: Acceleration of the ocean warming from 1961 to 2022 unveiled by large-ensemble reanalyses, *Nat. Commun.*, 15, 545, <https://doi.org/10.1038/s41467-024-44749-7>, 2024.
- Storto, A., Dobricic, S., Masina, S., and Di Pietro, P.: Assimilating Along-Track Altimetric Observations through Local Hydrostatic Adjustment in a Global Ocean Variational Assimilation System, *Mon. Weather Rev.*, 139, 738–754, <https://doi.org/10.1175/2010MWR3350.1>, 2011.
- Storto A, Masina, S., Balmaseda, M., Guinehut, S., Xue, Y., Szekely, T., Fukumori, I., Forget, G., Chang, Y.-S., Good, S. A., Köhl, A., Vernieres, G., Ferry, N., Peterson, K. A., Behringer, D., Ishii, M., Masuda, S., Fujii, Y., Toyoda, T., Yin, Y., Valdivieso, M., Barnier, B., Boyer, T., Lee, T., Gourrion, J., Wang, O., Heimbach, P., Rosati, A., Kovach, R., Hernandez, F., Martin, M. J., Kamachi, M., Kuragano, T., Mogensen, K., Alves, O., Haines, K., and Wang, X.: Steric sea level variability (1993–2010) in an ensemble of ocean reanalyses and objective analyses, *Clim. Dynam.*, 49, 709–729, <https://doi.org/10.1007/s00382-015-2554-9>, 2017.
- Storto, A., Bonaduce, A., Feng, X., and Yang, C.: Steric Sea Level Changes from Ocean Reanalyses at Global and Regional Scales, *Water*, 11, 1987, <https://doi.org/10.3390/w11101987>, 2019a.
- Storto, A., Alvera-Azcárate, A., Balmaseda, M. A., Barth, A., Chevallier, M., Counillon, F., Domingues, C. M., Drevillon, M., Drillet, Y., Forget, G., Garric, G., Haines, K., Hernandez, F., Iovino, D., Jackson, L. C., Lellouche, J.-M., Masina, S., Mayer, M., Oke, P. R., Penny, S. G., Peterson, K. A., Yang, C., and Zuo, H.: Ocean Reanalyses: Recent Ad-



- vances and Unsolved Challenges, *Front. Mar. Sci.*, 6, 418, <https://doi.org/10.3389/fmars.2019.00418>, 2019b.
- Storto, A., Masina, S., Simoncelli, S., Iovino, D., Cipollone, A., Drevillon, M., Drillet, Y., von Schuckman, K., Parent, L., Garric, G., Greiner, E., Desportes, C., Zuo, H., Balmaseda, M., and Peterson, K. A.: The added value of the multi-system spread information for ocean heat content and steric sea level investigations in the CMEMS GREP ensemble reanalysis product, *Clim. Dynam.*, 53, 287–312, <https://doi.org/10.1007/s00382-018-4585-5>, 2019c.
- Storto, A., Cheng, L., and Yang, C.: Revisiting the 2003–18 Deep Ocean Warming through Multiplatform Analysis of the Global Energy Budget, *J. Climate*, 35, 4701–4717, <https://doi.org/10.1175/JCLI-D-21-0726.1>, 2022.
- Sun, Y., Ditmar, P., and Riva, R.: Observed changes in the Earth's dynamic oblateness from GRACE data and geophysical models, *J. Geod.*, 90, 81–89, <https://doi.org/10.1007/s00190-015-0852-y>, 2016.
- Tapley, B. D., Bettadpur, S., Ries, J. C., Thompson, P. F., and Watkins, M. M.: GRACE measurements of mass variability in the Earth system, *Science*, 305, 503–505, <https://doi.org/10.1126/science.1099192>, 2004.
- Tibshirani, R.: Regression shrinkage and selection via the lasso, *J. Roy. Stat. Soc. B*, 58, 267–288, 1996.
- Tibshirani, R.: The LASSO method for variable selection in the Cox model, *Statist. Med.*, 16, 385–395, [https://doi.org/10.1002/\(SICI\)1097-0258\(19970228\)16:4<385::AID-SIM380>3.0.CO;2-3](https://doi.org/10.1002/(SICI)1097-0258(19970228)16:4<385::AID-SIM380>3.0.CO;2-3), 1997.
- Tsimplis, M. N. and Josey, S. A.: Forcing of the Mediterranean Sea by atmospheric oscillations over the North Atlantic, *Geophys. Res. Lett.*, 28, 803–806, <https://doi.org/10.1029/2000GL012098>, 2001.
- Volkov, D. L., Baringer, M., Smeed, D., Johns, W., and Landerer, F. W.: Teleconnection between the Atlantic Meridional Overturning Circulation and Sea Level in the Mediterranean Sea, *J. Climate*, 32, 935–955, <https://doi.org/10.1175/JCLI-D-18-0474.1>, 2019.
- Wong, A. P. S., Wijffels, S. E., Riser, S. C., Pouliquen, S., Hosoda, S., Roemmich, D., Gilson, J., Johnson, G. C., Martini, K., Murphy, D. J., Scanderbeg, M., Bhaskar, T. V. S. U., Buck, J. J. H., Merceur, F., Carval, T., Maze, G., Cabanes, C., André, X., Poffa, N., Yashayaev, I., Barker, P. M., Guinehut, S., Belbéoch, M., Ignaszewski, M., Baringer, M. O., Schmid, C., Lyman, J. M., McTaggart, K. E., Purkey, S. G., Zilberman, N., Alkire, M. B., Swift, D., Owens, W. B., Jayne, S. R., Hersh, C., Robbins, P., West-Mack, D., Bahr, F., Yoshida, S., Sutton, P. J. H., Cancouët, R., Coatanoan, C., Dobbler, D., Juan, A. G., Gouרון, J., Kolodziejczyk, N., Bernard, V., Bourlès, B., Claustre, H., D'Ortenzio, F., Le Reste, S., Le Traon, P.-Y., Rannou, J.-P., Saout-Grit, C., Speich, S., Thierry, V., Verbrugge, N., Angel-Benavides, I. M., Klein, B., Notarstefano, G., Poulain, P.-M., Vélez-Belchí, P., Suga, T., Ando, K., Iwasaka, N., Kobayashi, T., Masuda, S., Oka, E., Sato, K., Nakamura, T., Sato, K., Takatsuki, Y., Yoshida, T., Cowley, R., Lovell, J. L., Oke, P. R., van Wijk, E. M., Carse, F., Donnelly, M., Gould, W. J., Gowers, K., King, B. A., Loch, S. G., Mowat, M., Turton, J., Rama Rao, E. P., Ravichandran, M., Freeland, H. J., Gaboury, I., Gilbert, D., Greenan, B. J. W., Ouellet, M., Ross, T., Tran, A., Dong, M., Liu, Z., Xu, J., Kang, K., Jo, H., Kim, S.-D., and Park, H.-M.: Argo Data 1999–2019: Two Million Temperature-Salinity Profiles and Subsurface Velocity Observations From a Global Array of Profiling Floats, *Front. Mar. Sci.*, 7, 700, <https://doi.org/10.3389/fmars.2020.00700>, 2020.